 CMC, vol.53, no.2, pp.91-108, 2017

A Machine Learning Approach for MRI Brain Tumor Classification

Ravikumar Gurusamy[1] and Dr Vijayan Subramaniam[2]

Abstract: A new method for the denoising, extraction and tumor detection on MRI images is presented in this paper. MRI images help physicians study and diagnose diseases or tumors present in the brain. This work is focused towards helping the radiologist and physician to have a second opinion on the diagnosis. The ambiguity of Magnetic Resonance (MR) image features is solved in a simpler manner. The MRI image acquired from the machine is subjected to analysis in the work. The real-time data is used for the analysis. Basic preprocessing is performed using various filters for noise removal. The de-noised image is segmented, and the feature extractions are performed. Features are extracted using the wavelet transform. When compared to other methods, the wavelet transform is more suitable for MRI image feature extraction. The features are given to the classifier which uses binary tree support vectors for classification. The classification process is compared with conventional methods.

Keywords: MRI image, brain pathology, K-Means algorithm, Feature extraction, Wavelet transform, SVM, Neural network, K nearest algorithm.

1 Introduction

For medical diagnosis, image processing plays a vital role for analysis of brain images. Most methods are computerized and segmentation does the role in diagnosis, surgical planning, navigation and various medical evaluations. Segmentation is carried out using manual, semi-automatic and automatic methods. Automatic segmentation of MRI is important for the diagnosis of diseases and pathology. Clinical applications and scientific research depend on recent advancements in image processing. Segmentation separates the different tumor tissues such as necrotic cores, active cells and edema from normal brain tissues of white matter (WM). Extraction of gray matter (GM), and cerebrospinal fluid (CSF) was done by specialized methods. Noninvasive MRI based brain tumor segmentation was successful, since magnetic resonance imaging (MRI) images show the soft tissue contrasts effectively. This feature is not possible in X-ray images. A hybrid approach for brain tumor detection and classification through magnetic resonance images was proposed in literature [Praveen, Anita (2015)]. In this paper noise filtering was performed as a preprocessing

[1] Assistant Professor / ECE, Vivekanandha Institute of Engineering and Technology for Women Elayampalam, Tiruchengode, Namakkal(Dt) – 637205.
[2] Principal, Surya Engineering College, Mettukkadai, Erode – 638107.

stage on the image followed by skull detection. Then, MR brain images are subjected to feature extraction using a gray level co-occurrence matrix. After this extraction stage, and based on image features, classification is performed to classify normal or abnormal events using the Least Squares Support Vector Machine classifier. The kernel function used was the multilayer perception kernel. Even though this method was effective, clustering uncertainties remains a challenging task [Kong, Deng, and Dai (2015)]. When information theoretic learning was considered robust discriminative segmentation, methods looks effective but with tradeoffs on uncertainty avoidance because it simultaneously extracts the features and avoids the uncertainty [Liu, Li, Wang, et al. (2014)].

The uncertainties happen if the pooling data acquired through scanners are not clear. The data read from scanners should detect more subtle effects related to pathologies [Auzias, Takerkart and Deruelle (2015)]. But the influence of confounds or errors remains unclear. For example, in Autism Spectrum Disorders (ASD) diagnosis the influence of the scanner on age-related effects also to be observed Nicolas Cordier et al [Cordier, Delingette, Ayache (2015)] proposed a novel and generic approach for brain tumor segmentation using multi-atlas patch-based polling techniques. The conventional patch-based framework was enhanced in the paper through an improvement of the training dataset, intensity statistics, and invariance to cube isometries. The reported probabilistic model automatically delineates regions of tumor volumes with minimum running time and resources.

In Dong, Honnorat, Gaonkar, et al. (2015) a novel probabilistic clustering approach for modeling the pathological process by a combination of multiple regularized transformations from normal/control population to the patient population was proposed. In this paper the normal and patient populations are considered as point distributions. The reported MAP optimization was used for clustering the patients into groups and identifying disease subtypes. Huang et al [Huang, Yang, Wu, et al. (2014)] proposed a tumor segmentation method and a local independent projection-based classification (LIPC) method. Classification of voxel into different classes was done using local independent projection. A softmax regression model was proposed for data distribution of different classes. In Jiu, Zhang, Xiong, et al. (2015) extraction of component using 3-dimensional non-rigid registration and deformation modeling technique was used. The reported method can measure lateral ventricular (LaV) deformation in the volumetric magnetic resonance (MR) images. Karimaghaloo et al [Karimaghaloo, Rivaz, Arnold, et al. (2014)] presented an enhanced pathology segmentation method based on conditional Random Field (CRF) classifier. Lesion segmentation in brain Magnetic Resonance Images (MRI) was addressed by developing a Temporal Hierarchical Adaptive Texture CRF (THAT-CRF) method. The presented method was applied to the Images with Multiple Sclerosis (MS). In Kharratl, Halimal, Kharratl (2015) the authors presented a feature extraction method using Spatial Gray Level Dependence Matrix with discrete wavelet transform. The feature size was reduced using Simulated Annealing (SA) and the over fitting was avoided using Stratified K-fold Cross.

Kim et al [Kim, Lenglet, Duchin, et al. (2014)] proposed Volumetric segmentation of sub cortical structures like basal ganglia and thalamus. Complementary edge information in the multiple structural MRI modalities was utilized. Localization method for multiple pelvic bone structures on magnetic resonance images to localize pelvic bone structures automatically is done [Sinan, Susana, Paul, et al. (2014)]. Bone structures, however, are

not easily differentiable from soft tissue on MRI as their pixel intensities tend to be very similar. A support vector machine (SVM) and non-linear regression is utilized to identify the bounding boxes of bone structures on MRI. The presented model identifies the location of the pelvic bone structures by establishing the association between their relative locations and using local information such as texture features. Apart from these literatures several methods are proposed in past. Identification of gliomas [Pereira, Pinto, Alves et al. (2016)] using Convolutional Neural Networks (CNN) was presented in literature. For efficient analysis priori knowledge and biologically plausible model [Sudre, Jorge, Bouvy, et al. (2015)] of pathological data adaptable to subject's individual presentation will do better in diagnosis. Statistical methods with prior knowledge like principal component analysis (PCA) can be used to reduce the dimensionality of the feature space [Kharmega, Balamurugan (2014)] and assess cardiac kinetics in clinical practice [Viateur, Laurent, Thomas, et al. (2015)]. Discriminative Feature-oriented Dictionary Learning (DFDL) methods were adapted [Vu, Mousavi, Monga, et al. (2015)] to analyse histopathological images [Xing, Xie, and Yang (2015)].

2 MRI image preprocessing-noise removal

The MRI Recognition system consists of stages like image acquisition, denoising, preprocessing, segmentation, feature extraction and matching. Noise significantly corrupts the MRI image in the detection machine. During acquisition, the MRI image is corrupted by various noises like Salt and pepper, Gaussian, and speckle noise. High quality images can be obtained by denoising those corrupted images. Normally the conventional methods used in the machine removes the noise present in the signal. The occurrence of noise will substantially degrade the diagnostic effectiveness and requires a great level of subjectivity in the interpretation of the MRI images. Each method used in the MRI denoising has its own advantages and disadvantages. Many methods been developed for eliminating noises based on statistical property and frequency spectrum distribution. Noise is introduced at all stages of the image acquisition unit. The noises are Gaussian or non-Gaussian which happens due to several reasons. The signal and the noise are statistically independent of each other. Removal of noise from an MRI image is the one of the important tasks in the MRI recognition system.

The denoising techniques remove the noises and preserve the edges of an MRI as much as possible. There are various kinds of filters available for removing the noise from the MRI and different filters have their own characteristic. There are various denoising methods that are classified into spatial filtering and transform domain filtering. The spatial domain filtering further divided into linear and non-linear filtering. Generally linear techniques are used because of its speed of removing noise. But its limitation is that the linear technique does not preserve edges of images in efficient manner. On the other hand, nonlinear technique can handle edges of images in much better way than linear one. And, the non-linear filtering is used to remove such an impulsive noise. The spatial filtering method includes Gaussian filter, mean filter, median filter, Weiner filter, hemimorphic filter, SRAD (speckle reducing anisotropic diffusion) etc. In this work a detail investigation of the noise removal techniques like spatial noise filters which are further classified into linear filters and nonlinear filters, Discrete Cosine Transform, block-

wise non-local mean, optimized nonlocal means and wavelet based methods. The linear filters are arithmetic mean filter, geometric mean filter, harmonic mean filter and contra harmonic mean filter. The arithmetic filters are better than geometric filters since the latter blurs the image. The Gaussian noise in the MRI can be removed using the arithmetic and geometric filters since they remove random noise in an efficient way. For the removal of pepper noise nonlinear filters like max-min can be used but the dark pixels from the MRI image will be removed which contains the useful information. So nonlinear filters are not recommended when dark pixels are present in the image. Once noise is removed, MRI image enhancement is done to sharpen the tumor edges. To find the exact location and size of tumor, edge detection filters like spatial filters based on spatial differentiation, Sobel, Gaussian, Prewitt and Laplacian filter are applied in literature. The image obtained will have highlighted edges and discontinuities. But the Laplacian filter output is not an enhanced image it needs to be subtracted from the original image to obtain the sharpened enhanced image. From the investigation of methods, it's been found that a single methodology will not give a better result. Hybrid methods are providing successful enhancement.

Even though past research is being carried out vastly, Image denoising still remains a challenge for researchers because the noise removal process itself will introduce artifacts and causes blurring of the images. The focus is on wavelet transform, discrete wavelet transforms, biorthogonal wavelet filter, Haar wavlet, Coiflet, orthogonal wavelet filter, Symlet wavelet filter, log gobar filter, etc. comes under discrete domain transform provides effective MRI image denoising.

2.1 Types of noises

2.1.1 Salt and pepper noise (Impulse noise)

The salt and pepper noise which are impulse noise caused by the malfunctioning and fault memory locations and in the channel used for transmission. For MRI images corrupted by salt-and-pepper noise the noisy pixels deter a maximum or minimum random value. The salt-and-pepper noise in the image are either black or white. An image with salt-pepper noise is having either black pixel (value 0) in white region or while pixel (value 1) in dark region. From the literature we can find that the median filter was the popular nonlinear filter for removing impulse noise because of its good denoising power and computational efficiency. Median filter is used in the basic image processing system to remove salt-and-pepper noise because of its less sensitiveness compared with other linear techniques. At the same time, it will not affect the sharpness of the image. However, when the SNR level is only 50, the image details and edges are smeared by the filter itself losing some of the information. As MRI recognition system is used in security systems the noise should be completely removed without losing the image information. The probability density function for salt and pepper noise is given by equation 1:

$$PDF_{salt\&pepper} = \begin{cases} A & for \quad g = a("pepper") \\ B & for \quad g = b("salt") \end{cases} \tag{1}$$

2.1.2 Gaussian noise

As the name indicates, this type of noise adds a Gaussian distributed noise value to the

original pixel value, which has a bell-shaped probability distribution function given by the equation 2:

$$PDF_{Gaussian} = \frac{1}{\sqrt{2\pi\sigma}} e^{-\frac{(g-u)^2}{2\sigma^2}} \quad (2)$$

Where, g is the gray level, μ is the mean and σ is the standard deviation. The probability density function for Gaussian noise is shown in figure 3. Approximately 70% of the values are contained between $\mu \pm \sigma$ and 90% of the values are contained between $\mu \pm 2\sigma$. Although, theoretically speaking, the PDF is non-zero everywhere between -∞ and +∞, it is customary to consider the function 0 beyond $\mu \pm 3\sigma$.

2.1.3 Speckle noise

Speckle noise is a multiplicative noise and occurs in almost all coherent imaging systems such as laser, acoustics and SAR (Synthetic Aperture Radar) imagery. The source of this noise is attributed to random interference between the coherent returns. Fully developed speckle noise has the characteristic of multiplicative noise. Speckle noise follows a gamma distribution and is given as

$$F(g) = \frac{g^{\alpha-1}}{(\alpha-1)!\,\alpha^{\alpha}} e^{-\frac{g}{\alpha}} \quad (3)$$

Where a is variance and g is the gray level.

2.2 Image quality (performance) metrics

There is a variety of image quality measures available to compare various image processing algorithms. Using these measures, we can compare the original image (reference image) with the denoised image whose quality must be measured. The dimensions of the original image and the denoised image must be identical. The most common measures used are PSNR, MSE, CoC, SSIM and FSIM. In this paper, PSNR and MSE are used for measuring the image quality.

2.2.1 Peak signal to noise ratio (PSNR)

PSNR gives the ratio between possible power of a signal and the power of corrupting noise present in the image.

$$PSNR = 10\log_{10}\left[\frac{L^2}{MSE}\right] \quad (4)$$

where L is the dynamic range of the image, Ex. for 8-bit image, L=255.

2.2.2 Mean squared error (MSE) or root mean squared error (RMSE)

The root-mean-square deviation (RMSD) or root-mean-square error (RMSE) is a measure of differences between values predicted by a model and the values observed.

$$MSE = \frac{1}{MN}\sum_{i=1}^{M}\sum_{j=1}^{N}\left(I_{(i,j)} - J_{(i,j)}\right)^2 \quad (5)$$

Where I and J are images of size M X N.

2.3 Proposed denoising methodology

Since wavelet based denoising algorithms (uses soft or hard thresholding) provides smoothness and better edge preservation, the proposed technique uses wavelet domain as a primary technique**.** The wavelet domain with filter (shown in figure 1) will reduce the noise and produces better quality.

We are having various choices of spatial filters as well as wavelets. In the proposed system, at stage 1, median filter is used and in second stage symlet wavelet is used for filtering.

Stage 1-Filter Type 1 (Spatial Filter):

At stage 1, a non-linear filter like Median (suited for removing Salt & pepper Noise) and linear filters like Weiner (suited for removing Speckle noise) filters has been selected for filtering.

Stage 2-Filter Type 2 (Wavelet Transform)

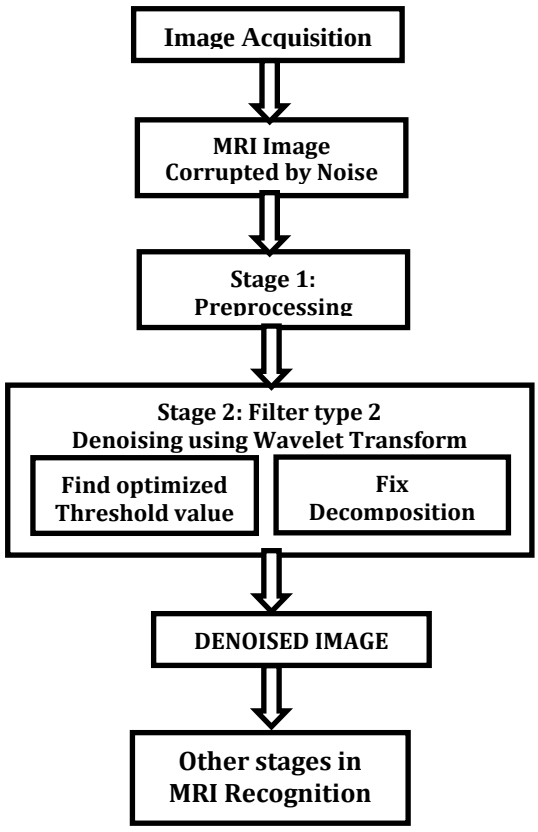

Figure1: Flow of proposed denoising Technique

The denoising techniques differ from each other only in the selection of the mother wavelets and number of decomposition levels. The image got from filter 1 is split into 4 sub bands, namely the HH, HL, LH and LL sub bands. The HH sub band gives the diagonal details of the image, HL sub band gives the horizontal features, LH sub-band represents the vertical structures and LL sub band is the low-resolution residual consisting of low frequency components and it is this sub-band which is further split at higher level of decomposition. There are several types of threshold namely hard, soft, semi-soft and semi-hard. Among them, the soft threshold has been selected because it gives aesthetically pleasing images as compared to the hard threshold. It will shrink the wavelet coefficients whose values are less than the threshold value and keeps all the wavelet coefficients whose values are larger than threshold value.

Table 1: PSNR values for denoising salt and pepper, Gaussian and speckle noise.

S.NO	TECHNIQUE	PSNR Salt & pepper Noise,	PSNR Gaussian Noise	PSNR Speckle Noise
1	MEDIAN FILTER	27	24	27
2	COIFLET1	22	27	30
3	SYMLET	21	26	29
4	WEINER	23	24	25
	SYMLET+WEINER	23	24	28
5	COIFLET + WEINER	24	24	27
6	SYMLET+MEDIAN	23	24	26
7	COIFLET + MEDIAN	23	24	26
8	PCA –Local Grouping	32	33	34

Table 2: PSNR values de-noising using the wavelet transform for various thresholding methods

S.NO	TECHNIQUE NAME /THRESHOLD	PHHT	FTHT	BSNHT	PHMT
1	Symlet55	25	23	20	24
1	COIFLET55	29	27	27	26
3	COIFLET55+WEINER	28	26	26	23
4	COIFLET55+MEDIAN	27	26	26	24

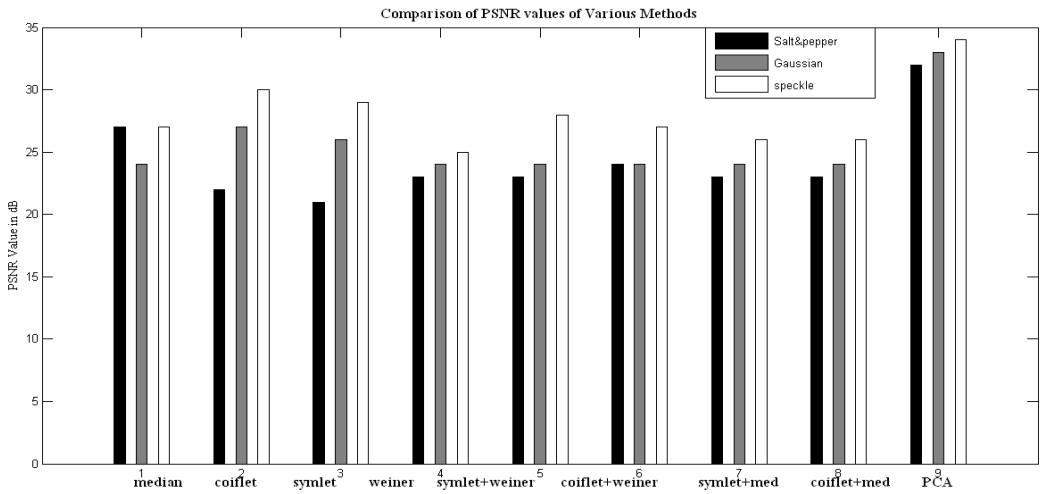

Figure 2: Comparison graph of PSNR of different

3 MR image (MRI) segmentation

Medical image segmentation labels each voxel in a medical image dataset to specify its tissue type and anatomical structure. The objective of segmentation is to present more affluent information in the original medical, to improve the visualization of the medical images and allows quantitative measurements of image structures. The segmentation is used for the quantification of tissues, classification (white matter, gray matter and cerebrospinal fluid of brain), diagnostic radiology, Localization of abnormalities, malfunctions, and pathologies. Prior to neurosurgery neuro imaging is done for decision making process for therapy and planning of neurological interventions. Brain tumor segmentation are classified into three category namely Manual segmentation, Semiautomatic segmentation and Fully automatic segmentation.

In manual segmentation are done through manually marking the area of interest or drawing the boundaries of the tumor. Anatomic structures with different labels are marked for diagnosis. The main complexity in manual delineation is that sophisticated graphical user interfaces are required. In addition, the tumor region selection was a time consuming and tedious work. On the other hand, manual based delineation is widely used in clinical trials. Since in clinical trials, a lot of human knowledge and expertise is required to distinguish tissues，it has been widely used. For semiautomatic brain tumor segmentation, the inputs and outputs are controlled manually. In the case of fully automatic methods the diagnosis program is within the acquiring machine so the diagnosis of tumor without any human interaction was carried out. The algorithms are inbuild with human intelligence based algorithms like machine learning approach and decision-making modules. Interpretability and transparency is the main requirement of the segmentation process. In this paper semiautomatic segmentation of brain tumors is presented which has least human interaction.

4 Proposed image pre-processing and feature extraction

4.1 Get an image get from database

In this paper work, real-time images from different databases are used for image classification and segmentation. The steps followed in the proposed work are given below.

Step 1. Pre-processing –denoising the MRI image.

Step 2. Feature extraction;

Step 3. Segmentation

Step 5. Training the kernel SVM;

Step 6. Testing with MRI brains.

Before feature extraction Otsu Binarization and K-Means clustering is performed.

In this paper we present the pre-processing, feature extraction and segmentation. The work presented in this paper is given in figure 3.

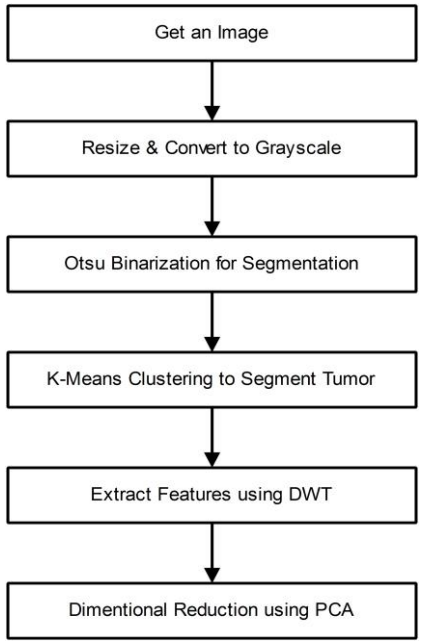

Figure 3: Steps involved in the feature extraction and reduction

4.2 Otsu binarization

The gray level image data is reduced to binary image and clustering based image thresholding is performed by Otsu's binarization method. The principle behind Otsu algorithm is bi-modal histogram and separates the two classes through optimized thresholding which has minimal intra-class variance. The threshold which minimizes the inter class variance is searched. The weighted sum of variances of the two classes is defined by

$$\sigma_{\omega}^2(\mathrm{T}) = \omega_0(\mathrm{t})\sigma_0^2(\mathrm{t}) + \omega_1(\mathrm{t})\sigma_1^2(\mathrm{t}) \quad (6)$$

$$\sigma_{\omega}^{2}(\mathrm{T}) = \omega_{0}(\mathrm{t})\sigma_{0}^{2}(\mathrm{t}) + \omega_{1}(\mathrm{t})\sigma_{1}^{2}(\mathrm{t}) \tag{7}$$

Where

ω –probability of the two class. The probabilities are separated by the threshold. The probability is computed from the histogram. It is calculated through iteration.

σ –variance of class. Mean and variance are computed through iteration.

Minimizing the intra-class variance was same as maximizing inter-class variance. In this work, the Otsu method improves the binarization process.

4.3 K-means (KM) clustering

Different clustering methods are proposed in literature like ISODATA, fuzzy C-mean and probabilistic C-means algorithm. Among this K-means clustering is the simplest to implement and to run. The clustering is based on portioning method. When compared to other algorithm its simple in its iteration process.

KM algorithm based clustering is utilized for the clustering of MRI dats. The algorithm is given below.

1. k cluster centers are chosen such that to coincide with chosen patterns inside the hyper volume which are chosen randomly containing the pattern set of the MR image. (C)

2. Assign each MRI pattern to the closest cluster center. (Ci, i = 1,2, ... C)

3. Recompute the cluster centers using the current cluster memberships. (U)

4. Chose a new cluster If a convergence criterion is not attained. minimal decrease in squared error.

$$\begin{cases} 1 \text{ if } \left\| \mathrm{x_j} - \mathrm{C_i} \right\|^2 \le \left\| \mathrm{x_j} - \mathrm{C_k} \right\|^2, \text{for each } \mathrm{k} \ne \mathrm{i} \\ 0 \text{ otherwise} \end{cases} \tag{8}$$

$$\mathrm{C_i} = \frac{1}{\left|\mathrm{G_i}\right|} \sum_{\mathrm{k}, \mathrm{x_k} \in \mathrm{G_i}} \mathrm{x_k} \tag{9}$$

Where, |Gi| is the size of Gi

Or

$$\left|\mathrm{G_i}\right| = \sum_{\mathrm{j=1}}^{\mathrm{n}} \bigcup_{\mathrm{ij}} \tag{10}$$

The MRI cluster center's initial positions decide the performance of the k means clustering algorithm. Since the MR image data is inherently put into iterative the convergence towards an optimum solution is different. But the convergence is reached by the K means algorithm through three steps until the stable is reached. Initially the centroid coordinates are determined followed by the distance measurement between each object and the centroid finally the object grouping is done based on the minimum distance.

4.4 Feature extraction

Wavelet transform based feature extraction from MR brain images is done. The advantage of

using it for images is that for various levels of resolution the details can be obtained. the MR image time and frequency information are preserved through time scale view which is advantageous when compared to time –frequency view.

The wavelet Algorithm has following steps:

1. Decide number of decomposition level.

In the proposed, the number of decomposition level is fixed as 3 because too much of decomposing will affect the quality of the MR image and it will be difficult to do the diagnosis.

2. Calculate the DWT of the image.

The DWT of any signal is calculated using the following formula.

$$S_{DWT}(j,k)=\sum_{n=0}^{N-1} S_n\, j, kw_n, \quad a=2^j, \tau=k2^j \tag{11}$$

Where Sn= s(nT) Signal samples

J, kWn= n^{th} sample of k^{th} sifted version of a 2j scaled discrete wavelet.

N = number of signal samples

3. Find an optimized value for Threshold.

There are four types of threshold namely hard, soft, semi-soft and semi-hard. Among them in this work soft threshold has been selected because it gives visually pleasant images while comparing with hard threshold. The soft threshold shrinks the wavelet coefficients below the threshold value while the wavelet coefficients larger than threshold value kept as such.

$$\begin{cases} sgn(w_{j,k}).(|w_{j,k}|-\lambda), & |w_{j,k}|\geq\lambda \\ 0, & |w_{j,k}|<\lambda \end{cases} \tag{12}$$

$\lambda = \sigma\sqrt{2\ln(N)}$

σ = median (|c|)/0.6745

Finding an optimum threshold value is tedious process and wrong selection will affect the quality of the denoised MRI image. Choosing a proper threshold will reduce the noisy content and avoids the removal of required signal.

4. Compute the IDWT to get the denoised estimate.

$$s_n=\frac{1}{N}\sum_{j=0}^{\log_2 N}\sum_{k=0}^{\text{int}(N/2^{j+1})} S_{j,k}\, j, kw_n \tag{13}$$

Where J,KWn = nth sample of k^{th} sifted version of a 2j scaled discrete wavelet,

J, K= row index and n = column index.

The feature extraction represents the original data in an alternate way by measuring certain properties or features that distinguish one input pattern of brain image from another pattern. Using the extraction process eight different textural features are analysed and given as input to different classifiers. The textural features extracted are angular second moment, contrast, correlation, variance, entropy, inverse difference Moment,

skewness and kurtosis.

4.5 Feature metrics

1. Angular Second Moment (ASM):

Named as energy of date in otherwise is represented in the equation.14.

$$f_1 = \sum_i \sum_j \{p(i, j)\}^2 \tag{14}$$

Where p(i,j) is the input image probability matrix. The energy will be maximum for MRI images with unequal intensity values.

2. Contrast:

The feature measures the image contrast and is expressed in equation.15.

$$f_2 = \sum_{n=0}^{N_{g-1}} n^2 \left\{ \sum_{i=1}^{N_g} \sum_{j=1}^{N_g} p(i, j) \right\} \tag{15}$$

Where Ng is the number of gray levels. The value is low for pixels with similar intensity.

3. Correlation:

The feature represents the linear dependency of grey levels on the neighboring pixels. Equation 16 represents the correlation between the two variables in statistical terms.

$$f_3 = \frac{\sum_i \sum_j (ij) p(i, j) - \mu_x \mu_y}{\sigma_x \sigma_y} \tag{16}$$

Where μ is the mean of input image in row –x and column-y.

σ is the standard deviations of the input image in the row-x and column-y.

4. Variance:

Variance measures the gray level spread out in the MRI image.

$$f_4 = \sum_i \sum_j (i - \mu)^2 p(i, j) \tag{17}$$

Where μ is the mean of the whole image.

5. Inverse Difference Moment (IDM**):**

Inverse difference moment is expressed in equation.18 representing smoothness of the image. Image with different gray levels of the pixel have less IDM.

$$f_5 = \sum_i \sum_j \frac{1}{1 + (i - j)^2} p(i, j) \tag{18}$$

6. Entropy:

Entropy represents the randomness of an image gray level distribution. The entropy value will be high if the gray levels are distributed randomly.

$$f_6 = -\sum_i \sum_j p(i,j)\log(p(i,j) - \mu)^3 \quad (19)$$

7. Skewness:

The measure of symmetry is given in equation.20.

$$f_7 = \frac{1}{\sigma^3} \sum_i \sum_j (p(i,j) - \mu)^3 \quad (20)$$

Skewness can be a negative or positive value. For symmetrical images value is zero.

8. Kurtosis:

Kurtosis is a measure of peaked or flatness of data relative to the normal distribution.

$$f_8 = \frac{1}{\sigma^4} \sum_i \sum_j (p(i,j) - \mu)^3 - 3 \quad (21)$$

5 Proposed image classification algorithm

Classification of basic features using different classifiers like Neural Networks, K-Nearest Neighbor and Naïve Bayes algorithm are investigated and compared with Binary Tree classifier. The extracted QRS amplitude and Heart rate features are given to the different classifier and trained. For testing different data set is given and checked. The performance is given in Table. 3. In this work a binary tree SVM classifier is proposed for the classification of the features. A Support Vector Machine (SVM) is a popular classifier which has self-learning features, dimensionally and space independent. SVMs are feed forward network with a single layer of non-linear units show accurate results with high efficiency. In addition, the SVM is proved to have minimized the structural risk for implementation. SVM minimizes the bound on the errors made by the learning machine over the data used for testing. The objective function of the training datasets can't be minimized. The SVM can able to classify perfectly the images that do not belong to training data. Classifications of data in training are done using support vectors. For difficult data set the SVM places the hyper plane which separates the difficult data into two classes using support vectors. The features obtained from the previous stage are classified using the proposed classifier.

6 Results and discussion

The analysis and results of the proposed methods are done using MATLAB. The execution results of the proposed method are given below step by step.

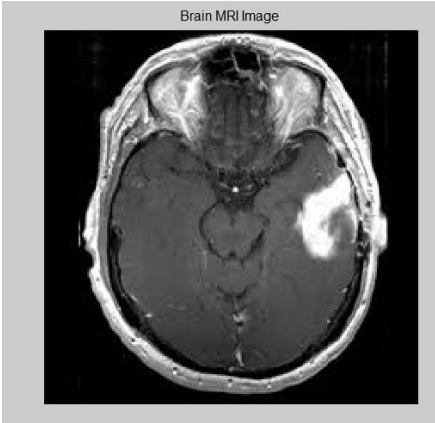

Figure 4: Input image used for analysis

Figure 4 shows the image under test for the proposed analysis. Figure 5,6,7 shows the results of the image after binarization, clustering and segmentation respectively. DICOM images are used for analysis.

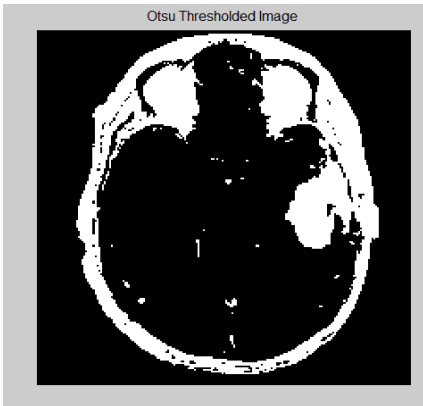

Figure 5: Output image after binarization

An example of features extracted are listed below for the image given in figure 1.

Contrast = 0.2433

Correlation = 0.1294

Energy = 0.7606

Homogeneity = 0.9344

Mean = 0.0034

Standard Deviation = 0.0897

Entropy = 2.9949

RMS = 0.0898

Variance = 0.0081

Smoothness = 0.9270
Kurtosis = 7.6801
Skewness = 0.6318
IDM = 0.3816
Figure 8 shows the Classifier Output images for diagnosing benign and malignant tumors.

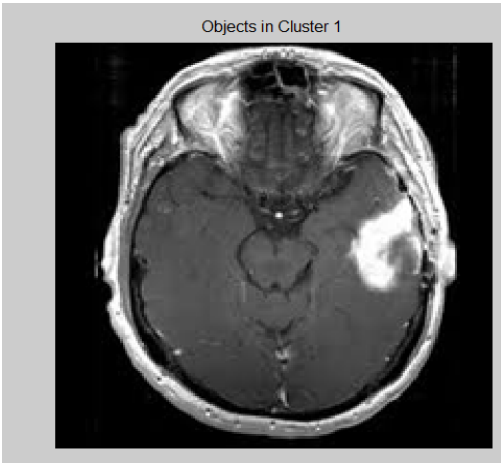

Figure 6: Output image after K means Clustering

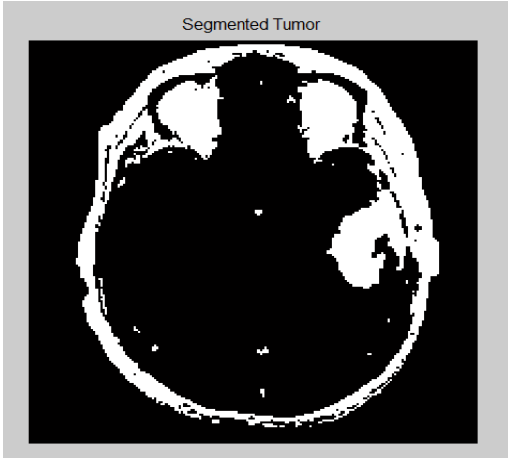

Figure 7: Output image with segmented tumor

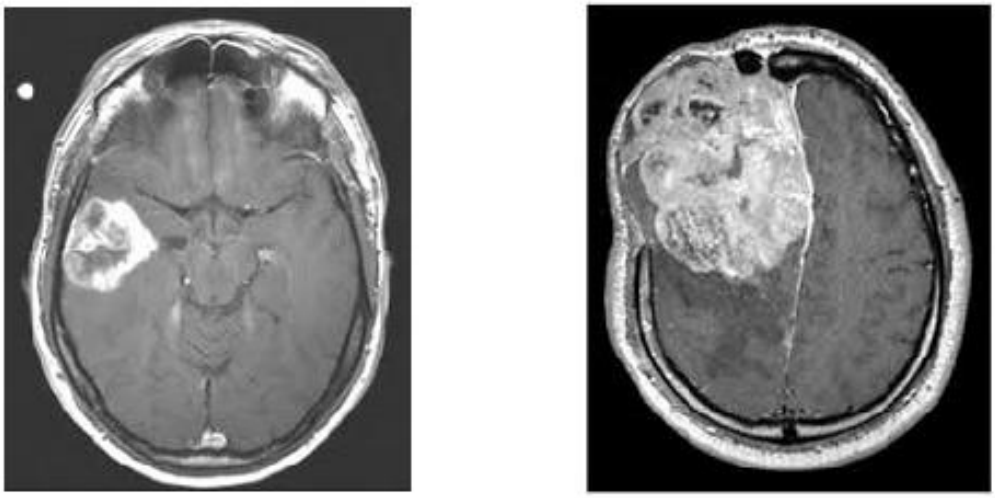

(a) (b)

Figure 8: Classifier Output image as **a) benign, b) malignant**

Table 3: Performance of the classifier

Classifier	Positive Predictive Value	Negative Predictive Value
Neural Network	97	97
KNN	96	96
Naive Bayes	89.21	93.7
Proposed SVM	98	98

From the Table 3 its been observed that the Neural network, KNN and proposed method gives more than 96% performance in the positive predictive and negative predictive value. The number of features given to the classifier is 8. The classification was done to diagnose

7 Conclusions

In this paper we have preprocessed and extracted the features of the MRI images. The database collection is one of the significant aspects of this paper. Both real-time images and simulated images are used in this project which is an added advantage. Secondly, an extensive pre-processing technique is employed to remove the unwanted noises. The success rate of this step is high which has guaranteed the overall accuracy of the system. Finally, an optimal feature set is extracted from these images which are very important for performance enhancement of the automated system. Since the convergence rate is also one of the performance measures of this work, the number of features used in this work is not too high to avoid any computational complexity. In future the classification algorithm will be framed using proposed SVM method.

References

Auzias, G.; Takerkart. S.; Deruelle, C. (2015): On the Influence Confounding Factors in Multi-site Brain Morphometry Studies of Developmental Pathologies: Application to Autism Spectrum Disorder. *IEEE Transactions on Medical Imaging JBHI-00050-2015*, pp.1-8.

Cordier, Nicolas; Delingette, Herv ́e; Ayache, Nicholas. (2015): A patch-based approach for the segmentation of pathologies: Application to glioma labeling. *IEEE Transactions on Medical Imaging*, vol.35, no.4, pp.1-11.

Dong, Aoyan; Honnorat, Nicolas,; Gaonkar, Bilwaj; Davatzikos, Christos. (2015): CHIMERA: Clustering of heterogeneous disease effects via distribution matching of imaging patterns. *IEEE Transactions on Medical Imaging*, pp.1-10.

Huang, Meiyan; Yang, Wei; Wu, Yao; Jiang, Jun; Chen, Wufan; Feng, Qianjin. (2014): Brain Tumor Segmentation Based on Local Independent Projection-based Classification. *IEEE Transactions on Biomedical Engineering*, pp.1-13.

Jui, Shang-Ling; Zhang, Shichen; Xiong, Weilun; Yu, Fangxiaoqi; Fu, Mingjian; Wang, Dongmei; Hassanien, Aboul Ella; Xiao, Kai. (2015): Brain MR Image Tumo Segmentation with 3-Dimensional Intracranial Structure Deformation Features. *IEEE*

INTELLIGENT SYSTEMS, pp.1-9.

Karimaghaloo, Zahra; Rivaz, Hassan; Arnold, Douglas L.; Louis Collins, D.; Arbel, Tal. (2014): Temporal Hierarchical Adaptive Texture CRF for Automatic Detection of Gadolinium-Enhancing Multiple Sclerosis Lesions in Brain MRI. *IEEE Transactions on Medical Imaging*, pp.1-16.

Kharmega Sundararaj, G.; Balamurugan, V. (2014): Robust Classification of Primary Brain Tumor in Computer Tomography Images Using K-NN and Linear SVM. *Proceedings of International Conference on Contemporary Computing and Informatics (IC3I)*, pp.1315-1319.

Kharratl, Ahmed,; Halimal, Mohamed Ben. (2015): MRI Brain Tumor Classification using Support Vector Machines and Meta-Heuristic Method. *Proceedings of 15th International Conference on Intelligent Systems Design and Applications (ISDA)*, Marrakech, Morocco, pp.446-451.

Kim, Jinyoung; Lenglet, Christophe; Duchin, Yuval; Sapiro, Guillermo; Harel, Noam (2014): Semiautomatic Segmentation of Brain Subcortical Structures From High-Field MRI. *IEEE JOURNAL OF BIOMEDICAL AND HEALTH INFORMATICS*, vol.18, no.5, pp.1678-1695.

Kong, Youyong; Deng, Yue; Dai, Qionghai. (2015): Discriminative Clustering and Feature Selection for Brain MRI Segmentation. *IEEE SIGNAL PROCESSING LETTERS*, vol.22, no.5, pp.573-577.

Liu, Jin; Li, Min; Wang, Jianxin; Wu, Fangxiang; Liu, Tianming; Pan, Yi. (2014): A Survey of MRI-Based Brain Tumor Segmentation Methods. *TSINGHUA SCIENCE AND TECHNOLOGY ISSNll1007-0214ll04/10*, vol.19, no.6, pp.578-595.

Onal, Sinan; Lai-Yuen, Susana; Bao, Paul; Weitzenfeld, Alfredo; Hart, Stuart (2014): Automated Localization of Multiple Pelvic Bone Structures on MRI. *IEEE Journal of Biomedical and Health Informatics*, pp.1-7.

Pereira, Sergio; Pinto, Adriano; Alves, Victor; Silva, Carlos A. (2016): Brain Tumor Segmentation using Convolutional Neural Networks in MRI Images. *IEEE Transactions on Medical Imaging*, vol.35, no.5, pp.1240-1251.

Praveen, G. B.; Agrawal, Anita. (2015): Hybrid Approach for Brain Tumor Detection and Classification in Magnetic Resonance Images. *Proceedings of International Conference on Communication, Control and Intelligent Systems (CCIS)*, Mathura, India. pp.162-165,

Sudre, Carole, H.; Jorge Cardoso, M.; Bouvy, Willem; Biessels, Geert J.; Barnes, Josephine; Ourselin, Sebastien. (2015): Bayesian model selection for pathological neuroimaging data applied to white matter lesion Segmentation. *IEEE Transactions on Medical Imaging*, vol.34, no.10, pp.2079-2102.

Tuyisenge, Viateur; Sarry, Laurent; Corpetti, Thomas; Innorta-Coupez, Elisabeth; Ouchchane, Lemlih; Cassagnes, Lucie. (2015): Estimation of Myocardial Strain and Contraction Phase from Cine MRI using Variational Data Assimilation. *IEEE Transactions on Medical Imaging*, vol.35, no.2, pp. 442-455.

Vu, Tiep Huu; Mousavi, Hojjat Seyed; Monga, Vishal; Rao, Ganesh; Rao, Arvind.

(2015): Histopathological Image Classification using Discriminative Feature-oriented Dictionary Learning. *IEEE Transactions on Medical Imaging*, vol.35, no.3, pp.738-751.

Xing, Fuyong; Xie, Yuanpu; Yang, Lin. (2015): An Automatic Learning-based Framework for Robust Nucleus Segmentation. *IEEE Transactions on Medical Imaging*, vol.35, no.2, pp.550-566.